CEAS Aeronautical Journal
https://doi.org/10.1007/s13272-022-00626-x

ORIGINAL PAPER

Evaluation of the controllability of a remotely piloted high-altitude platform in atmospheric disturbances based on pilot-in-the-loop simulations

Yasim J. Hasan[1] · **Mathias S. Roeser**[1] · **Andreas E. Voigt**[1]

Received: 24 February 2022 / Revised: 24 October 2022 / Accepted: 2 November 2022

Abstract
In the context of the project HAP, the German Aerospace Center (DLR) is currently developing a solar-powered high-altitude platform that is supposed to be stationed in the stratosphere for 30 days. The development process includes the design of the aircraft, its manufacturing and a flight test campaign. Furthermore, a high-altitude demonstration flight is planned. While the high-altitude flight will be performed using a flight control and management system, during take-off and landing and at the beginning of the low-altitude flight test campaign, the aircraft will be remotely piloted. The aircraft has a wing span of 27 m and operates at extremely low airspeeds, being in the magnitude of around 10 m/s equivalent airspeed, and is therefore profoundly susceptible to atmospheric disturbances. This is particularly critical at low altitudes, where the airspeed is lowest. Hence, both time and location for take-off, landing or low-altitude flight test campaigns need to be selected thoroughly to reduce the risk of a loss of aircraft. In this regard, the knowledge about the operational limits of the aircraft with respect to atmospheric conditions is crucial. The less these limits are known, the more conservative the decision about whether to perform a flight on a certain day or not tends to be. On the contrary, if these limits have been adequately investigated, the amount of days and locations that are assessed as suitable for performing a flight might increase. This paper deals with a pilot-in-the-loop simulation campaign that is conducted to assess the controllability of the high-altitude platform in atmospheric disturbances. Within this campaign, the pilots are requested to perform practical tasks like maintaining track or altitude, flying a teardrop turn or performing a landing while the aircraft is subject to different atmospheric disturbances including constant wind, wind shear, continuous turbulence, and discrete gusts of different magnitudes. This paper describes the desktop simulator used for the campaign, outlines the entity of investigated test points and presents the assessment method used to evaluate the criticality of the respective disturbances. Finally, a set of restrictions on the acceptable wind conditions for the high-altitude platform are found. The underlying limits comprise a constant wind speed of 3.0 m/s in any direction, except during landing, maximum wind shear of 0.5 m/s^2 and gusts with peak speeds of 1.5 to 2.0 m/s, depending on the direction.

Keywords High-altitude platform · Flight mechanics · Pilot-in-the-loop simulations · Atmospheric disturbances · Desktop simulator

List of symbols

a, b, c	Distances
C_l	Coefficient of flow separation function
C_L	Lift coefficient
C_n	Yawing moment coefficient
C_Y	Side force coefficient
h	Altitude
h_1	Reference altitude
H	Transfer function
N	Number of samples
L	Scale length
r	Horizontal lever arm
R	Radius
s	Frequency parameter
S	Area
V_{NE}	Never-exceed speed
$V_{O,max}$	Maximum operating speed
$V_{O,min}$	Minimum operating speed
V_S	Stalling speed
X	Separation point

✉ Yasim J. Hasan
yasim.hasan@dlr.de

[1] Institute of Flight Systems, German Aerospace Center (DLR), Lilienthalplatz 7, 38108 Braunschweig, Germany

Published online: 15 November 2022

Greek symbols

α	Angle of attack
$\dot{\alpha}$	Time derivative of angle of attack
α^*	Turning point angle of attack of flow separation function
β	Angle of sideslip
ζ	Rudder deflection
σ	Standard deviation
τ	Time constant

Indices

dyn	Dynamic
SW	Sidewash
u,v,w	Velocity components in x-, y- and z-directions
W	Value for wind
WB	Value for wing-body

Abbreviations

AVL	Athena Vortex Lattice
6DOF	Six-Degrees-Of-Freedom
DLR	Deutsches Zentrum für Luft- und Raumfahrt (German Aerospace Center)
HAP	High-altitude platform
HTP	Horizontal tailplane
LAPL(A)	Light aircraft pilot license (aeroplane)
PPL	Private pilot license
SAR	Synthetic aperture radar
SPL	Sailplane pilot license/sport pilot license
TPI	Task performance indicators
VTP	Vertical tailplane

1 Introduction

During the last 2 decades, the research on so-called high-altitude platforms (HAPs, *sg.* HAP) has increased significantly [1–5]. HAPs are air vehicles designed to operate at high altitudes, mainly in the lower stratosphere, and mostly for a relatively long time. If driven by solar power, HAPs can stay airborne for several weeks [6]. This prolonged operating time together with the high operation altitude makes HAPs suitable candidates for a variety of applications that otherwise lie in the scope of satellite usage. These applications include general earth observation missions [7], e.g. surveillance in case of humanitarian crises or natural catastrophes, and telecommunications [8]. Compared to satellites, HAPs have the advantages of a higher flexibility in use since they are not dependent on their orbit, and of a closer proximity to the ground bringing benefits with respect to image resolution.

The long operating time imposes challenging demands on the design and the operation of solar-powered HAPs. Since the power provided by the solar cells and the storage capacity of the batteries are limited, the flight needs to be as efficient as possible. On the one hand, for fixed-wing HAPs this leads to the need for a very high aerodynamic efficiency and very low structural weight. On the other hand, this requires a relatively low airspeed at the design point, being at high altitudes. However, this implies that the airspeed at low altitudes is particularly low. As a consequence, small wind perturbations already lead to large changes in the aerodynamic angles and to significant track deviations. Altogether, the flight in low altitudes as, e.g. during take-off and landing constitutes a serious risk for a loss of aircraft. This is also reflected by a couple of mishaps involving HAPs that encountered atmospheric disturbances. One example is the NASA Helios aircraft that encountered a shear line over Hawaii in 2003 which led to divergent aeroelastic effects and finally to an in-air break-up of the aircraft [9]. Another example is an Airbus Zephyr 8 aircraft that entered an area of unstable atmospheric conditions over Australia in 2019. The turbulences caused uncommanded roll reactions of the aircraft leading to a high bank angle which the aircraft could not be recovered from. This resulted in a spiral descent whereupon the aircraft broke apart [10].

To reduce the risk of a loss of aircraft, it is thus crucial to select the time and the location for flights that involve low altitudes, for at least a part of the time, thoroughly. However, only a small subset of days of the year are expected to show sufficiently adequate weather conditions, such that a safe flight can be performed. In this regard, the knowledge about the operational limits of the aircraft with respect to atmospheric conditions is crucial. The less these limits are known, the more conservative the decision about whether to perform the flight on a certain day or not tends to be. On the contrary, if these limits have been adequately investigated, the amount of days that are assessed as suitable might increase. Hence, an accurate knowledge about these limits enables a better flight planning and facilitates the choice of appropriate test locations.

The German Aerospace Center (DLR) is currently developing a HAP system in the context of the DLR-internal project *HAP*. The HAP system includes the aircraft itself, the flight control system and the full operational concept, the ground segment, the flight termination system and two instruments (payload) with a mass of up to 5 kg each. The two instruments, being a high-definition camera and a synthetic aperture radar (SAR), are interchangeable. Thus, the aircraft is designated to perform earth observation missions carrying one of these instruments depending on the use case. The aircraft development process is currently about to enter the detail design phase. The HAP aircraft has a total mass of about 140 kg, a wing span of 27 m and a wing area of 36 kg. Within the further project term, the manufacturing, a comprehensive flight test campaign and a final high-altitude mission demonstration using the instruments will follow. The flight test campaign is planned for summer 2024.

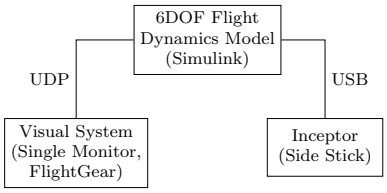

Fig. 1 Sketch of the desktop simulator environment

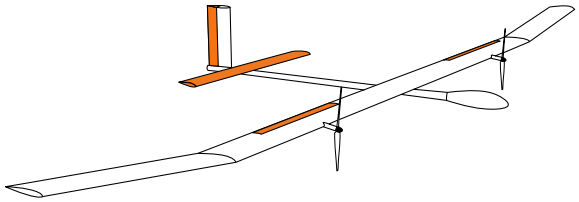

Fig. 2 Sketch of the DLR HAP aircraft

High-altitude flights will be performed using a flight control system. However, during take-off and landing, and at least at the beginning of the flight test campaign the HAP is supposed to be piloted remotely. To reduce the risks during these flight phases, it is therefore crucial to investigate the influences of atmospheric disturbances on the HAP's controllability taking into account the pilot's capabilities. This paper presents the pilot-in-the-loop simulations performed for this purpose. The general aims of this study are to identify the most critical wind conditions for different pilot tasks, to evaluate the controllability with respect to these tasks in a perturbed atmosphere and to define wind restrictions.

This paper starts with a description of the simulator environment in Sect. 2. Subsequently, Sect. 3 outlines the different test points, being combinations of pilot tasks and different wind conditions, investigated within the pilot-in-the-loop simulations. Furthermore, the general assessment method used within this work is explained in Sect. 4. Finally, this paper presents the results in Sect. 5 and closes with the conclusion and a short outlook in the Sects. 6 and 7.

2 Simulator environment

This section describes the general simulator environment. Within the works presented here, a desktop simulator with a simple infrastructure is used. This is due to the fact that the aircraft development process within the project currently is at a preliminary design status. Hence, the setup of a more detailed simulator is not yet possible. Nevertheless, the main purpose of the simulator is to obtain knowledge about the HAP as early as possible in the design phase, wherefore the quality of the present simulator is sufficient. Figure 1 shows the structure of the simulator environment. It consists of a 6-degrees-of-freedom (6DOF) flight dynamics model, which is implemented using MATLAB®/Simulink®. For the vision the visual system provided by the open-source simulator *FlightGear Flight Simulator* [11] is used and displayed on a single monitor. The data exchange between the flight dynamics model and the visual system is realised via the User Datagram Protocol (UDP). Both the model and *FlightGear* are run on the same computer. For pilot inputs a side-stick without hinge moment-dependent force feedback is used, which is connected to the computer via the USB (Universal Serial Bus) interface. No acoustic feedback is provided.

2.1 Flight dynamics model

The flight dynamics model forms the core of the simulator environment. It has been continuously enhanced during the different design stages of the project *HAP*. It includes geometry, aerodynamic, structural, and aeroelastic data provided by the complete flight physics team in the project.

2.1.1 The DLR HAP aircraft

Figure 2 shows a sketch of the DLR HAP aircraft. It is an ultralight aircraft with high aspect ratio and dihedral in the outer wing sections. Its payload bay is located in the aircraft front section. The aircraft is equipped with two propeller engines and has two ailerons, an all moving horizontal stabiliser and a rudder. The aircraft has a total mass of around 140 kg, a wing span of 27 m and a wing area of 36 m^2.

The aircraft's flight envelope is defined by four characteristic airspeeds, which are mainly based on the aeroelastic design speeds, as described in [12], being:

- **Stalling speed** V_S (6.5 m/s at sea level): Stall occurs below this airspeed. The airspeed shall never fall below this speed.
- **Minimum operating speed** $V_{O,min}$ (9.0 m/s at sea level): This is the lower limit of the operation envelope. During normal operation, excluding take-off and landing, the airspeed should not be lowered deliberately below the operating minimum speed. Nevertheless, externally provoked excursions, e.g. due to gusts, are acceptable.
- **Maximum operating speed** $V_{O,max}$ (11.0 m/s at sea level): This is the upper limit of the operation envelope and thus should not be exceeded deliberately.
- **Never-exceed speed** V_{NE} (15.5 m/s at sea level): This airspeed shall never be exceeded, otherwise structural damages might occur.

2.1.2 Aerodynamics model

In the flight dynamics model, the aircraft aerodynamics is modelled using aerodynamic derivatives as described in [13]. Nevertheless, in [13] a two-point aerodynamic model was used for the longitudinal motion to separate the influences of wing-body (including the payload bay) and horizontal tailplane (HTP). This signifies that the aerodynamic forces and moments are calculated for these points separately. For the lateral-directional motion, a one-point aerodynamic model is used, i.e. the derivatives are given for the complete aircraft. For this work, however, the lateral-directional aerodynamic model was also enhanced to a two-point-model, separating wing-body and the vertical tailplane (VTP).

2.1.3 Stall models

The flight dynamics model includes two stall models, one for the wing and one for the VTP. Wing stall is modelled using an approach that considers the flow separation point at the main wing due to the angle of attack as introduced by [14]. Herein, the angle of attack-dependent portion of the wing-body (WB) lift coefficient is reduced by a factor that represents the degree of flow separation:

$$\left(C_{\mathrm{L_{WB}}}\right)_{\alpha} = C_{\mathrm{L}\alpha_{\mathrm{WB}}} \cdot \alpha \cdot \left(\frac{1+\sqrt{X}}{2}\right)^2. \tag{1}$$

Here, X is the non-dimensional separation point ranging from 0 to 1. It can be modelled using a couple of modelling parameters as

$$X = \frac{1}{2} \cdot \left[1 - \tanh\left(C_1 \cdot (\alpha - \tau\dot{\alpha} - \alpha^*)\right)\right], \tag{2}$$

where C_1 is a coefficient, τ is a time constant and α^* is the angle of attack at which the flow separation function has its turning point. Note that this modelling approach does not account for HTP stall, especially if it occurs due to high pitching rates. Therefore, during the evaluation of the test points, the time histories of the HTP angle of attack are additionally checked and it is verified that maximum allowable values are not exceeded[1].

Stall effects at the VTP are considered by using the VTP side force curves for different rudder deflections ζ and directly calculating the VTP side force with the local sideslip angle β_{VTP}. Due to the small lever arm of the VTP, the effects are not included in the rolling motions. The respective coefficients for side force C_{Y} and yawing moment C_{n} yield:

$$\begin{aligned} C_{\mathrm{Y}} &= C_{\mathrm{Y_{WB}}} + \cos\left(\beta_{\mathrm{VTP}}\right) \cdot C_{\mathrm{Y_{VTP}}}(\beta_{\mathrm{VTP}}, \zeta) \cdot \frac{S_{\mathrm{VTP}}}{S} \\ C_{n} &= C_{\mathrm{n_{WB}}} + \cos\left(\beta_{\mathrm{VTP}}\right) \cdot C_{\mathrm{Y_{VTP}}}(\beta_{\mathrm{VTP}}, \zeta) \cdot \frac{S_{\mathrm{VTP}}}{S} \cdot r_{\mathrm{VTP}} \end{aligned} \tag{3}$$

Here, r_{VTP} is the horizontal VTP lever arm, S is the wing area and S_{VTP} is the VTP area. The VTP sideslip angle is given by

$$\beta_{\mathrm{VTP}} = \beta - \beta_{\mathrm{W}} + \beta_{\mathrm{W_{VTP}}} + \beta_{\mathrm{dyn}} + \beta_{\mathrm{SW}}, \tag{4}$$

where β_{W} is the main wing sideslip angle due to wind, $\beta_{\mathrm{W_{VTP}}}$ is the sideslip angle at the VTP due to wind and β_{dyn} is the dynamic sideslip angle at the VTP caused by a yawing motion. For the HAP aircraft, the sidewash angle is neglectable and thus $\beta_{\mathrm{SW}} \approx 0\,^{\circ}$.

2.1.4 Consideration of flexibility and limitation of this approach

As already mentioned, six degrees of freedom are considered in the flight dynamics model. The structural dynamics are not yet included. Instead, a dynamic pressure-dependent quasistatic approach is used. Herein, sets of aerodynamic derivatives are given for the four characteristic equivalent airspeeds presented in Sect. 2.1.1. For intermediate airspeeds, linear interpolation is performed at each time step during the simulation runtime. The aerodynamic derivatives are provided by the aerodynamics department as described in [13] and calculated using the vortex lattice method *Athena Vortex Lattice* (AVL) [15, 16] for the flight shapes at the respective airspeeds.

The HAP aircraft's wing deformation is still in the linear elastic regime but during level-flight, the wing tip vertical displacement is around 6 to 7% of the aircraft's semispan [17]. Figure 3 depicts the spanwise elastic deformation of wing and HTP in z-direction for the different airspeeds at sea level, which the derivatives are given for.

Using such an approach to account for flexibility, effects of the variation of the flight shape due to a change of equivalent airspeed are included. Hence, when the aircraft shows a

[1] In the context of this work, no attention is paid to HTP stall recovery. Instead, if the critical HTP angle of attack is exceeded, this is assumed as a flight condition that can not be recovered from. For the assessment of single test points, which will be described later, such a case is simply deemed as unacceptable. Therefore, the presented wing stall model is sufficient for this purpose. However, this is not the case for VTP stall. If stall occurs at the VTP, the wing-body aerodynamics have an effect that can assist in recovering from this condition. Such a condition can thus not be assumed as unacceptable per se. In addition, due to the low VTP aspect ratio, the VTP side force curve is not linear at low sideslip angles, where it would usually be linear. To cover these effects, VTP stall is modelled more thoroughly in these works.

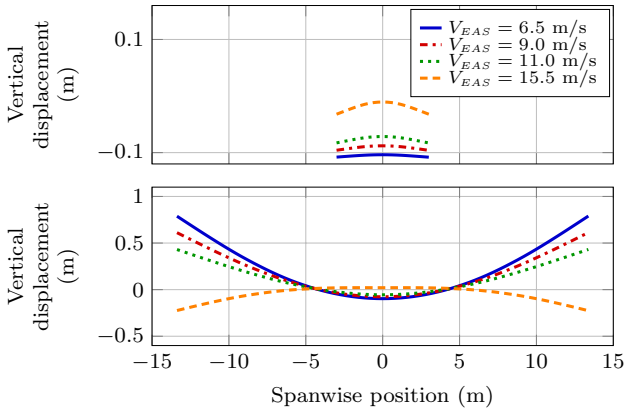

Fig. 3 Elastic deformation of wing and HTP in z-direction for different airspeeds at sea level

reaction to wind or control inputs during runtime, the change in airspeed leads to changes of the aerodynamic properties and the control surface effectivenesses.

However, this approach does not account for changes of the flight shape due to rotational rates or a changing load factor. In addition, cross-coupling effects between the aircraft's structural dynamics and its aerodynamics are not respected. In the context of the project *HAP*, these influences were respected in the context of the aeroelastics analysis and were investigated in detail [17].

Not including them in the pilot-in-the-loop simulations signifies that the interplay of the pilot, the aircraft's aerodynamics and structural dynamics can not be reproduced. Hence, the risk of effects like pilot-induced oscillations driven by the flexible dynamics cannot be assessed in this work. On the other hand, effects like adverse aerodynamic properties or insufficient control authorities due to high airspeed excursions can be assessed.

2.1.5 Turbulence model

Continuous turbulence is modelled for the translational wind components by passing white noise through a filter. The respective forming filters are such that approximate Von Kármán velocity spectra are obtained [18]. The corresponding transfer functions read:

$$
\begin{aligned}
H_u(s) &= \frac{\sigma_u \sqrt{\frac{L_u}{V}}\left(1 + 0.25\frac{L_u}{V}s\right)}{1 + 1.357\frac{L_u}{V}s + 0.1987\left(\frac{L_u}{V}\right)^2 s^2} \\
H_v(s) &= \frac{\sigma_v \sqrt{\frac{L_v}{V}}\left(1 + 2.7478\frac{L_v}{V}s + 0.3398\left(\frac{L_v}{V}\right)^2 s^2\right)}{1 + 2.9958\frac{L_v}{V}s + 1.9754\left(\frac{L_v}{V}\right)^2 s^2 + 0.1539\left(\frac{L_v}{V}\right)^3 s^3} \\
H_w(s) &= \frac{\sigma_w \sqrt{\frac{L_w}{V}}\left(1 + 2.7478\frac{L_w}{V}s + 0.3398\left(\frac{L_w}{V}\right)^2 s^2\right)}{1 + 2.9958\frac{L_w}{V}s + 1.9754\left(\frac{L_w}{V}\right)^2 s^2 + 0.1539\left(\frac{L_w}{V}\right)^3 s^3}.
\end{aligned}
\tag{5}
$$

Here, σ_u, σ_v and σ_w are velocity standard deviations for the different axes and L_u, L_v and L_w are the scale lengths. They are set as proposed in the certification specifications CS-AWO [19]. For low altitudes ($h < h_1$, while $h_1 = 1000$ ft), the scale lengths are

$$
\begin{aligned}
L_w &= h \\
L_u = L_v &= \frac{h}{\left(0.177 + 0.823\frac{h}{h_1}\right)^{1.2}}
\end{aligned}
\tag{6}
$$

and the relation between the standard deviations of the different axes is

$$
\sigma_u = \sigma_v = \frac{\sigma_w}{\left(0.177 + 0.823\frac{h}{h_1}\right)^{0.4}}.
\tag{7}
$$

At higher altitudes ($h > h_1$), the values for the scale lengths are equivalent for all axes:

$$
L_u = L_v = L_w = h_1.
\tag{8}
$$

The same is true for the standard deviations:

$$
\sigma_u = \sigma_v = \sigma_w.
\tag{9}
$$

Other types of wind perturbations like constant wind or discrete gusts are introduced into the flight dynamics model in form of external input.

2.2 Vision system

As already mentioned, the vision system consists of the *FlightGear* vision and some virtual instruments, both displayed on a single monitor. The view is body-fixed and it has its reference somewhat behind the VTP. The instruments are displayed using Simulink®. They are placed below the view of the aircraft and arranged side by side. Instruments are provided for airspeed, with the characteristic airspeeds presented in Sect. 2.1.1 highlighted, and bank angle, altitude, vertical speed, sideslip angle and thrust. Figure 4 shows a screenshot of the pilot view.

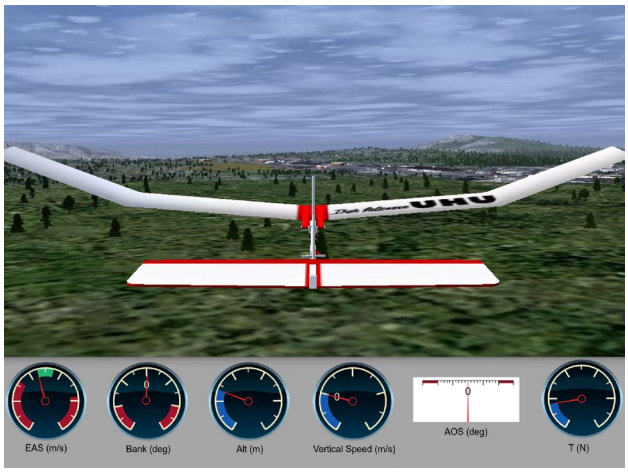

Fig. 4 Pilot view of the aircraft and the instruments; note that the mockup does not represent the DLR HAP aircraft

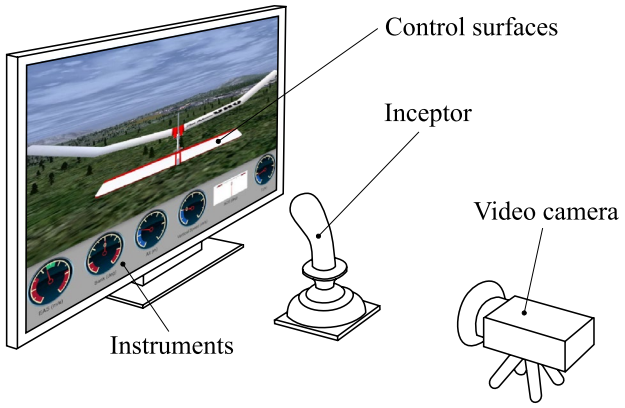

Fig. 5 Sketch of the latency measurement setup

2.3 Inceptor

A simple side-stick without hinge moment-dependent force feedback is used as inceptor. The side-stick is allocated such that roll inputs are applied by moving the side-stick to the left or to the right, pitch inputs are applied by moving it forward or rearward and yaw inputs are applied by twisting the side-stick. Engine RPM is controlled by a slide controller.

2.4 Latency measurements

Within the real flight, all signal paths will be associated with time lags, so-called latencies. For example, when the remote pilot applies a control input, the deflection first needs to be sampled and is then sent to the remote pilot station where it is processed by different types of communication modules. Afterwards, it is sent via an uplink connection to the HAP aircraft, where it is processed again by different computers until it is sent to the actuators, which finally realise the commanded control inputs. Since all these steps take a certain amount of time, there exists a latency between the pilot input and the actual control deflection. The same is true for the measurement signals that are obtained by the sensors on board, sent to the control station on ground and monitored there. Depending on the respective aircraft and the order of magnitude of the latencies, these latencies can lead to pilot-induced oscillations [20–22] or at least impede the pilot from assessing the current flight conditions properly. Therefore, latencies can bear a risk with respect to flight safety. For the flight test within the project *HAP*, maximum allowable latencies of 200 ms (desirably 100 ms) where defined both for the control latency (latency between pilot control input and control deflection at the aircraft) and monitoring latency (latency between a measurement on board and its indication in the ground station).

Within the desktop simulation, all signal paths are likewise associated with time lags. A control input using the inceptor is first sampled and then transferred to the simulation via USB where it is processed. The simulation output is either sent to the *FlightGear* vision system via UDP in case of the aircraft view or visualised by Simulink in case of the instruments. Even though pilot-induced oscillations are very unlikely to occur for the HAP aircraft due to its rather slow flight dynamics, it is reasonable to measure the latencies of the desktop simulator to be capable of better assessing the simulation results' significance for the real flight.

Latency measurements have been performed with the present desktop simulator both for the view itself and for the instruments. Figure 5 shows the general setup of these measurements. The inceptor was deflected to realise control surface deflections. For the latency measurements, the actuator dynamics of the flight dynamics model was deactivated. A video camera was used to record at the same time the inceptor deflection and both the visual geometric control surface deflections within the aircraft view and the reaction of an instrument, which the numerical deflection value of the stabiliser was fed into. The video was then post-processed using image processing techniques. In doing so, the frames where the inceptor was deflected the first time and those where the geometric control surfaces, respectively the instrument, showed a first reaction were detected. Using the number of frames between those and using the video frame rate, the latencies could then be calculated.

Figure 6 shows the respective results in form of box plots. In sum, 100 measurements have been made. As shown, latencies for the displayed instruments, having the median at around 300 ms, are slightly higher than for the view, whose median is roughly 200 ms. For the view, the maximum latency is around 500 ms and 75% of the data points lie below around 300 ms.

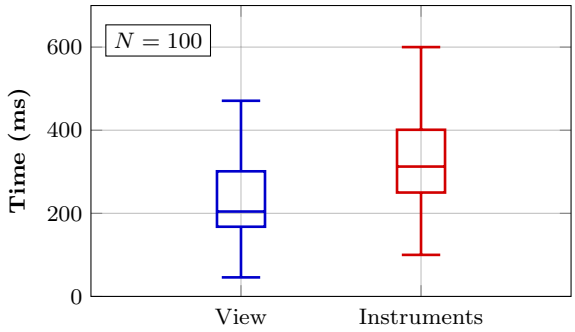

Fig. 6 Results of latency measurements

The instruments' latencies have maximum values of about 600 ms with 75% of the values below roughly 400 ms.

Note that for the desktop simulation, it was not possible to measure the control latency or the monitoring latency independently. Instead, the sum of both latencies were measured for the aircraft view and the instruments. The results, therefore, need to be compared to the sum of the defined maximum values for the real flight, which is 400 ms. The measurements for the simulator are thus of a similar size. Therefore, it can be concluded that, judging from the latencies, the desktop simulator is appropriate for the works presented in this paper.

2.5 Applicability of the simulator

While significant effort has been put into modelling the HAP aircraft's flight dynamic characteristics, other elements of the simulator are kept rather simple. This is particularly true for the vision system and the inceptor. In addition, no sound system providing acoustic feedback for the pilot was implemented. In sum, the flight conditions from a pilot point of view differ from those expected for the first flight test campaign. However, the aim of this study is the evaluation of the general feasibility of performing certain tasks with the HAP aircraft at different atmospheric conditions. Hereby, the focus is on the capabilities of the aircraft itself rather than on those of the pilot while considering the real flight conditions. Therefore, the quality and complexity of the desktop simulator is supposed to be sufficient for the investigations this paper covers. Nevertheless, it should be noted that the simulator is not applicable for pilot training. Instead, a more detailed simulator will be implemented within the project *HAP* for these purposes.

3 Test procedure

This section gives an overview of the investigated test points, presenting the different combinations of tasks and wind conditions. In addition, it presents the general approach followed during the execution of the tests.

3.1 Objective

The main aim of the works presented here is to investigate the influences of different wind perturbations on the HAP aircraft's remotely piloted flight. This includes the analysis of the general controllability of the aircraft in disturbed atmosphere, the identification of the most critical wind conditions and the definition of allowable wind limits for the flight in low altitudes.

3.2 Tasks and wind conditions

Every test point is a combination of a task and a wind condition. Four different tasks, being to maintain track, fly a teardrop turn, perform a landing and to maintain altitude, are to be performed by the pilots. At the same time, either constant wind, wind shear or a discrete gust of different direction and magnitude, or continuous turbulence in all three axes and of different magnitude are applied. In the context of this work, a rather analytical approach is pursued. To investigate the influences of different wind types separately, different wind types are not superimposed, even though the presence of strong rather constant wind is, in practice, most often accompanied by a higher degree of turbulence.

3.2.1 Tasks

This section describes the different tasks the pilots are requested to perform.

Maintain track

The main requirement of this task is, as the name says, to maintain the track during the flight. For this purpose, the aircraft is placed at an altitude of 100 m over ground above a runway. Its track is aligned with the runway to provide a visual reference for the pilot. It should be noted that, during this manoeuvre, the runway never left the field of vision displayed on the monitor, even though at large crosswinds large crab angles are necessary to maintain track. While lateral wind of different type is applied, the pilot is supposed to reduce the resulting track deviations using the available control surfaces and, if required, thrust. In doing so, the pilot is explicitly requested not to correct lateral offsets that build up thereafter.

Teardrop turn

The teardrop turn task, depicted in Fig. 7, is included in the programme since it represents a convenient manoeuvre with respect to the flight test campaign that is destined within the project *HAP*. During these tests, the HAP aircraft will be mainly operated by the so-called remote pilot, who is located in the nearby control station and watches the aircraft via a first person view camera. However, at the same

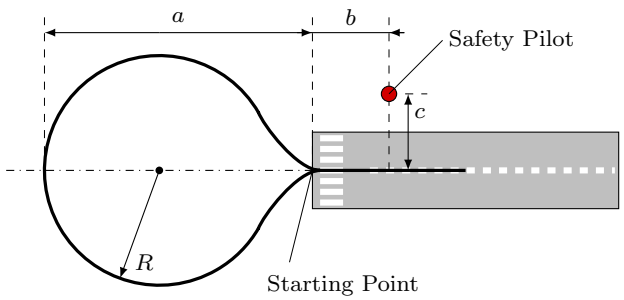

Fig. 7 Schematic representation of the teardrop turn task

time a safety pilot is located on the airfield, having a direct view of the aircraft. The latter is supposed to interact in case of emergencies. Therefore, the aircraft must not exceed a maximum distance of around 800 m to the safety pilot. This circumstance makes the teardrop turn more suitable than a conventional turn. During the simulator tests the aircraft is placed above and aligned with the runway. The manoeuvre starts as soon as the aircraft passes the runway threshold. The pilot is then supposed to fly a turn in such a way that he passes the starting point again but in the reverse direction.

Landing

Another task of the programme is a landing with transverse approach. Thereby, touchdown must occur in a designated landing area. The area is perceptible in the simulation since it is accentuated with a colour different from the surrounding terrain. The allowed landing area has an equivalent diameter of less than 100 m. The aircraft is placed at an altitude over ground of 50 m and with a distance of around 500 m from the landing area. It should be noted that the purposes of the investigation are solely to evaluate whether it is possible to reach the intended landing area in atmospheric disturbances or not and how difficult this is for the pilot. Therefore, no attention is paid to the actual realisation of the landing, e.g. execution of the flare.

Maintain altitude

For this task the aircraft is placed at an altitude of 100 m over ground. The pilot is supposed to attenuate the resulting altitude deviations due to different wind disturbances.

3.2.2 Wind conditions

Various wind conditions are applied during the tasks. Figure 8 shows the different types schematically. The directions are always chosen according to the respective task. Hence, for the maintain track task a lateral gust is applied, for instance, while for the maintain altitude task, the aircraft rather encounters a vertical or a head- or tailwind gust.

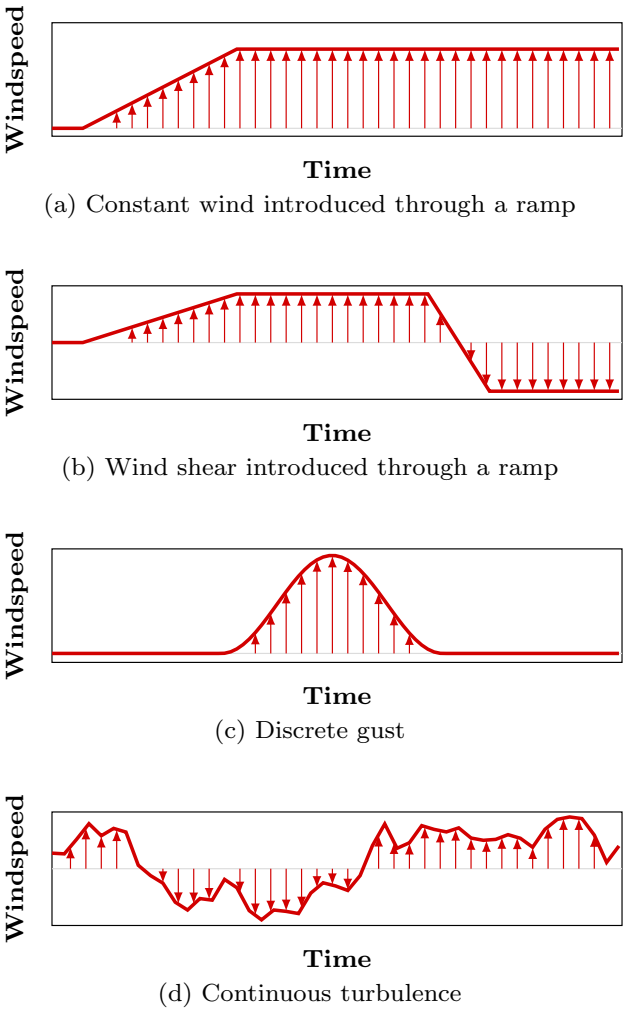

Fig. 8 Different types of wind applied within the simulator tests

Figure 8a shows how constant wind is applied. The flight starts without wind and after a certain time the wind occurs. The wind speed increases linearly until the target wind speed is reached. This speed is held constant.

The flight through wind shear is simulated as depicted in Fig. 8b. It is represented by a change of wind speed over time, rather than over a distance. Similarly to the case with constant wind, the wind is introduced in form of a ramp. The wind is then kept constant for quite some time until the wind speed changes linearly until it has the same magnitude but opposite direction.

Figure 8c shows the shape of a gust as applied within the simulator tests. The gust shape is defined as proposed in the EASA CS-25 [23] while the magnitude is reduced to account for lower wind speeds. Two different gust wave lengths, 33.5 m and 82.5 m, are investigated, as medium wavelengths have proven to be the most critical with respect to the HAP aircraft's controllability in foregoing investigations. Shorter gust lengths rather have an impact on structural sizing since

their impact time is shorter or at least similar to the pilot reaction time. Longer gusts lengths would particularly culminate in a flight through moving atmosphere, and thus neither are a controllability issue.

Continuous turbulence, as represented schematically by Fig. 8d, is applied to all three axes using the method described in Sect. 2.1.5.

3.3 Test points and execution

To define limits for acceptable wind conditions, it is not sufficient to only investigate one test point for each combination of tasks and wind conditions. Instead, the wind speed needs to be varied for each combination as well. Therefore, a high number of test points need to be included. However, depending on the respective result of a test point, another test point may become redundant. For instance, if a pilot fails to perform a task for a given wind condition, it is not reasonable to repeat the combination with a higher wind speed.

Furthermore, the HAP aircraft's flying qualities are rather unusual. Depending on a pilot's experience with such a type of aircraft, the learning effect might have an important influence on the results. To circumvent this factor, the order of test points was randomised.

Due to the reasons described above, the following approach is used for the execution of the simulator tests. For each combination of task and atmospheric disturbances, three different test points with lower, medium, and higher wind speeds are included. It is subdivided into three rounds for each pilot:

1. In the first round, all test points with medium wind speeds are executed while, among these test points, the order is chosen at random. For each test point, the simulation is run anew and the pilot is informed about the task. However, the pilot is only informed about the presence of continuous turbulence and constant wind, since during a real flight only this information would be available. This includes the initial constant wind phase for wind shear. However, the pilot does not have knowledge about whether a gust will occur or the wind direction changes. After a variable time wind occurs while the pilot performs the tasks. After having completed the task or having stabilised the aircraft, the test point is completed and the simulation is stopped. The pilot is then supposed to assess the feasibility of the task with the given wind condition using grades ranging from 1 to 5. The different grades are defined as follows:

   1: The task was easy to execute.
   2: The task had an acceptable level of complexity.
   3: There were minor control issues executing the task.
   4: There were major control issues executing the task.
   5: The difficulty of the task was not acceptable.

   Depending on the assessment, the test point of the same combination but with higher, respectively lower, wind speeds is chosen for the next rounds of the simulator test. Here, in the case of an assessment of 4 or 5 the combination of task and wind conditions is usually regarded as not acceptable. However, the distinction between easier and more complex tasks is not always based on the grade alone. Instead, the pilot is also asked to describe his perception of the test point and to state difficulties he encountered. In addition, the grade given by the pilot for this test point is also considered in relation to the grades given by the same pilot for the other test points. This way, the pilot's tendency to generally assess the feasibility as more difficult or vice versa is also respected. This approach and the grade system are used for every task in an equal manner. In some cases a single test point may be repeated.
2. In the second round, only those combinations that the pilot assessed as more complex are investigated. Therefore, the test points with lower wind speeds than in the first round are performed. The order is chosen at random again. After completion of each test point, the pilot again assesses the feasibility of the test points.
3. In the third round, the combinations in which the tasks could be more easily fulfilled, are investigated with increased wind speeds. The procedure is identical to the other rounds. Note that, depending on the remaining time, not all test points were always performed.

Figure 9 shows the distribution of the test points and Table 1 documents the associated wind speeds. Altogether, 114 test points were performed by three pilots.

3.4 Pilots

Three pilots participated in the test campaign. This section shortly specifies their backgrounds and piloting experience.

– Pilot 1: The first pilot has the light aircraft pilot license for aeroplanes LAPL(A) since September 2015. His experience covers around 285 flight hours with single engine piston airplanes, including several different aircraft types like the *Van's Aircraft RV-4*, the *Aquila A 210*, the *Robin DR 400* and more, and about 70 hours with touring motor gliders (*Fournier RF 5*). Furthermore, he has the German sport pilot license (SPL) for ultralight aircraft since July 2021 with 4 flight hours of experience flying the *Ikarus C42*. The pilot graduated in Aerospace Engineering, obtaining the Master of Science and thus has theoretical knowledge of flying and handling qualities assessment. Moreover, he participated in the flight

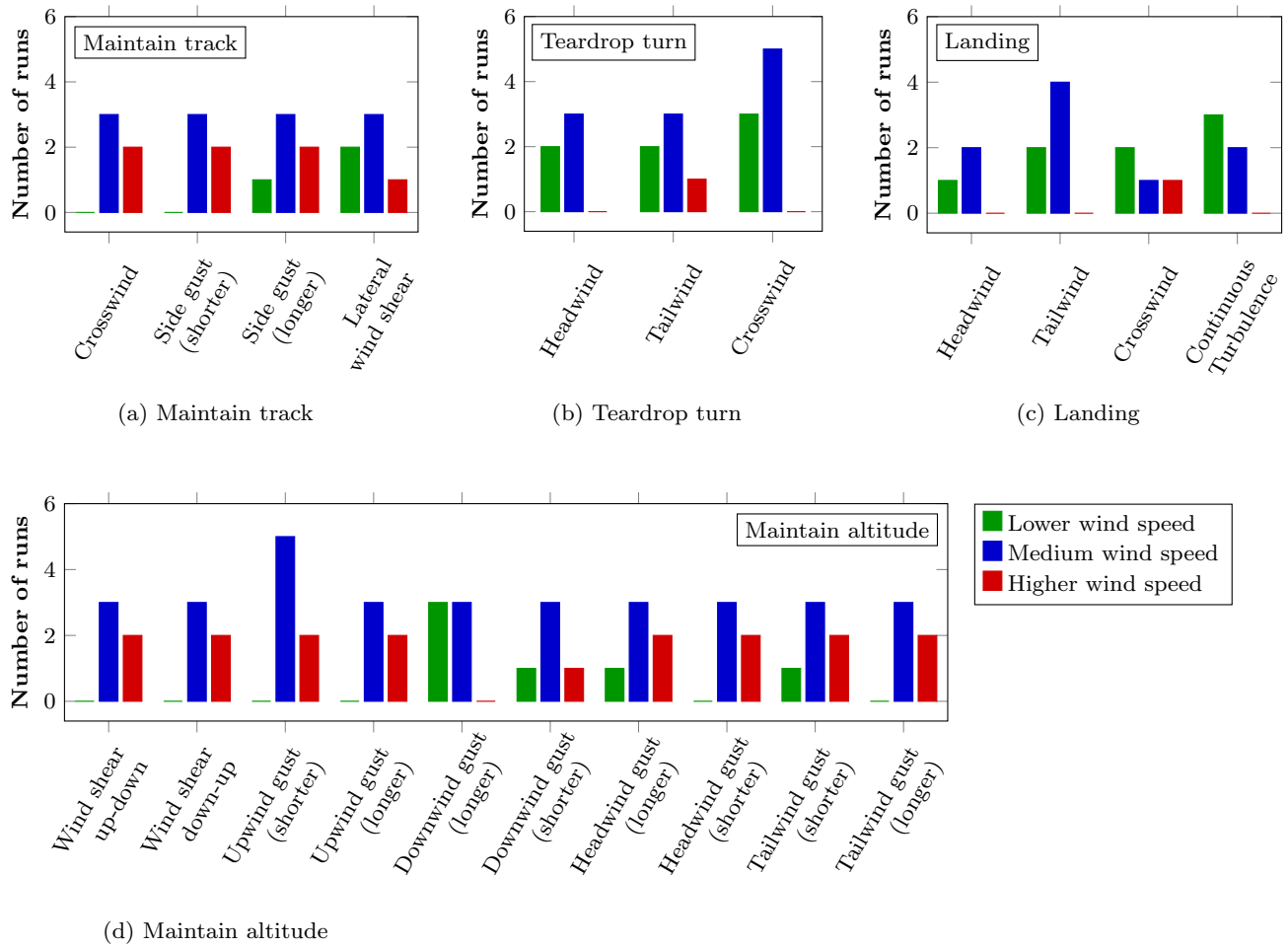

(a) Maintain track (b) Teardrop turn (c) Landing

(d) Maintain altitude

Fig. 9 Overall distribution of test points. While all pilots performed the test points with medium wind speeds in the first round, the election of test points for the following rounds are based on the pilot assessment during the first round. Therefore, the test point distribution is not uniform and some test points were not performed at all. In addition, only reasonable combinations of tasks and wind conditions, e.g. crosswind during the maintain track task rather than headwind, are investigated

testing of the *Van's Aircraft RV-7* including aerobatic flight.

- Pilot 2: The second pilot has the private pilot license PPL for aeroplanes with class rating for single engine land class aircraft up to 2 tons since 2011. He has around 120 flight hours of experience flying the *Aquila AT01* and the *Cessna 172*. In addition, he has the saiplane pilot license (SPL) since 1989. His experience covers around 1250 flight hours with the *Schleicher ASK 21*, the *Schleicher ASW 20*, the *Schleicher ASG 29* and the *Schempp-Hirth Standard Cirrus*. He graduated in Aerospace Engineering and has theoretical knowledge of flying and handling qualities assessment. In addition, due to his experience, his ability of assessing sailplane aircraft is comparatively high.
- Pilot 3: The third pilot flies model aircraft in his private life since 1995. He is employed at DLR as safety pilot for model aircraft since October 2019. His experience as DLR safety pilot covers around 20 flight hours, including 12 flight hours flying fixed-wing aircraft. He has the civil drone licenses A1/A3 and A2. In addition, he obtained the license to operate large aircraft and rotorcraft models with a mass of more than 25 kg in April 2021. This pilot is rather used to flying air vehicles from a third person view than from a first person view.

4 Assessment scheme

As described in the foregoing section, during the simulator tests, the pilots assess each test point by assigning grades from 1 to 5 with respect to the feasibility of the task. However, these evaluations are subjective and based on qualitative estimations and are therefore always dependent on the pilots' skills and background. Therefore, the grade system is not used for the final assessment of the test points. As

Table 1 Summary of test points with applied wind speeds

	Magnitude	Maintain altitude, wind type	Magnitude
Maintain track, wind type			
Crosswind	2.0 m/s	Wind shear up-down	0.5 m/s^2
	3.0 m/s		2.0 m/s^2
	5.0 m/s		5.0 m/s
Side gust (33.5 m)	1.1 m/s	Wind shear down-up	0.5 m/s^2
	3.3 m/s		2.0 m/s^2
	5.5 m/s		5.0 m/s^2
Side gust (82.5 m)	1.3 m/s	Upwind gust (33.5 m)	1.1 m/s
	3.8 m/s		3.3 m/s
	6.3 m/s		5.5 m/s
Lateral wind shear	0.5 m/s^2	Upwind gust (82.5 m)	1.3 m/s
	2.0 m/s^2		3.8 m/s
	5.0 m/s^2		6.3 m/s
		Downwind gust (82.5 m)	1.3 m/s
			3.8 m/s
Teardrop turn, wind type			6.3 m/s
Tailwind	1.0 m/s	Downwind gust (33.5 m)	1.1 m/s
	3.0 m/s		3.3 m/s
	5.0 m/s		5.5 m/s
Headwind	1.0 m/s	Headwind gust (82.5 m)	1.3 m/s
	3.0 m/s		3.8 m/s
	5.0 m/s		6.3 m/s
Crosswind	1.0 m/s	Headwind gust (33.5 m)	1.1 m/s
	3.0 m/s		3.3 m/s
	5.0 m/s		5.5 m/s
		Tailwind gust (33.5 m)	1.1 m/s
			3.3 m/s
Landing, wind type			5.5 m/s
Headwind	4.0 m/s	Tailwind gust (82.5 m)	1.3 m/s
	6.0 m/s		3.8 m/s
	8.0 m/s		6.3 m/s
Tailwind	1.0 m/s		
	2.0 m/s		
	3.0 m/s		
Crosswind	2.0 m/s		
	3.0 m/s		
	5.0 m/s		
Continuous turbulence	0.1 m/s		
	0.2 m/s		
	0.5 m/s		

described in Sect. 3.3, it serves only to decide whether the wind speeds for a task will be increased or decreased for the next rounds.

For the assessment another more quantitative assessment method is required that takes into account, whether allowable limits are exceeded or not. Furthermore, it must be applicable for the high amount of test points and should exclude influences of the learning effect and individual pilot experience as much as possible. For this purpose, so-called indicators are introduced.

4.1 Introduction of indicators

Three different types of indicators, being flight safety indicators, handling indicators, and task performance indicators are introduced, which are presented in the following.

Depending on the indicator type, multiple corresponding indicators are defined. Generally, these indicators indicate if afore-defined limits are exceeded. In this case, its value is set to 1. Otherwise, a value of 0 is assigned. The underlying limits are defined using engineering judgement based on expectable real flight conditions. Hence, it is expected that a safe flight can be performed with the HAP aircraft if all of the following limits are not exceeded.

The evaluation of a single test point using indicators is performed the following way: For each indicator type, all associated indicators are grouped together. Then, the percentage is calculated, with which indicators of this type have values of 1. Based on these percentages, the wind condition of this test point is assessed.

4.1.1 Flight safety indicators

The flight safety indicators represent a measure of the criticality of the flight at this point. In case of an excess of the underlying limits, there is a risk of a loss of aircraft. These following indicators are defined, which are each set to 1 if

- the airspeed once falls below $1.2 \cdot V_S$,
- the airspeed once exceeds $0.8 \cdot V_{NE}$, or
- maximum allowable rotation rates are exceeded.

The flight safety indicators represent a hard criterion. Hence, the wind condition at a test point is always classified as non-acceptable if at least one of the indicators is 1.

4.1.2 Task performance indicators (TPI)

The task performance indicators are used to assess the feasibility of the task. Thus, the indicator definitions depend on the respective tasks.

TPI for the maintain track task

The limits are:

- The maximum track deviation must not exceed 30°.
- The mean track deviation must not exceed 5°.

Otherwise, the respective indicators are set to 1.

TPI for the teardrop turn

In case of the teardrop turn, only the following limit is defined:

- The maximum radius of the turn must not exceed 300 m.

Indeed, other requirements, like, e.g. an offset to the starting point while returning, could be defined for this task. Nevertheless, with respect to the designated flight test campaign in the project *HAP*, only the maximum radius has a practical relevance. The chosen value results when assuming a maximum allowable distance from aircraft to safety pilot of 800 m. With an altitude of 100 m, and the lengths $a \approx 650$ m, $b \approx 100$ m and $c \approx 100$ m (compare Fig. 7), this yields a maximum allowable radius of roughly 300 m.

TPI for the landing

For the landing, the following limits are defined:

- Touchdown must occur in the allowable landing area (compare Sect. 3.2.1).
- The airspeed at the moment of touchdown must not exceed 10 m/s.
- The maximum bank angle at the moment of touchdown must not exceed 3°.

In case of an excess of these limits, the respective indicators are set to 1.

TPI for the maintain altitude task

During this task, the limits are

- maximum allowable loss of altitude of 10 m and
- maximum allowable gain of altitude of 20 m.

Otherwise, the respective indicators are set to 1.

4.1.3 Handling indicators

The handling indicators show how demanding the respective task is for the pilot. The indicators have values of 1

- if at least one control surface is deflected by more than 80% for more than 20% of the time,
- if at least one control surface is at its deflection limit continuously for more than 3 s,
- or if the airspeed is outside the operational envelope, defined by $V_{O,min}$ and $V_{O,max}$, for more than 20% of the time.

These indicators rather form a soft criterion, which is particularly used to support decision-making.

5 Results

This section deals with the results of the simulator study. It shows exemplary ground and flight paths for different tasks, documents resulting limits and demonstrates the assessment method with indicators using the example of the maintain track task.

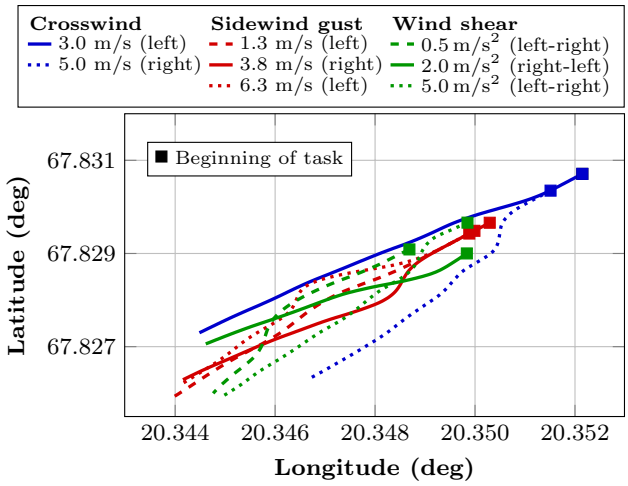

Fig. 10 Selected representative ground paths obtained during the maintain track task

5.1 Maintain track

First, the results for the maintain track task are presented here. Figure 10 shows some representative exemplary ground paths for this task. It should be noted that the time slices for each test point are cut such that only the relevant flight sections are used for calculation of the indicators. In doing so, the initial track value of the cut time slice (highlighted by filled squares and marked as beginning of task in the figure) is used as the reference for the maximum track deviation but the initial track of the complete time slice is used as reference for the mean track deviation. For gusts and constant wind, the section starts right before the first occurrence of wind. However, for wind shear the time slices are cut during the first phase of constant wind. The reason for this is that otherwise, the different phases of constant wind could compensate each other with respect to track deviations.

As shown in Fig. 10, constant winds mainly have an impact on the mean track deviation. In case of constant left wind with a magnitude of 3.0 m/s (blue, solid line) the aircraft has a slightly different track during the complete flight compared to the initial track. This is due to the fact that the pilot has some difficulties to perceive the aircraft's track because of the low airspeed. Gusts and wind shear have an impact on the maximum track deviation at first but also on the mean track deviation subsequently. In case of, for instance, the right side gust with a peak wind speed of 3.8 m/s (red, solid curve), the gust encounter starts at around 20.349° longitude and 67.829° latitude. The initial reaction is a track deviation to the left hand side. The pilot then starts to counteract the gust. However, as soon as the gust encounter ends (at around 20.349° longitude and 67.829° latitude), the aircraft tends to move to the other side both due to the aircraft reaction and due to the remaining pilot inputs. The associated track deviation then needs to be reduced, which takes quite some time for the pilot. It should be noted that the pilot is explicitly requested to not counteract resulting lateral offsets during this task. The maximum occurring lateral offsets were about 100 m.

In the following, the assessment method using indicators, as described in Sect. 4, is presented. Figure 11 illustrates this method. Figure 11a shows the resulting overall distribution of indicators for flight safety, task performance, and handling of the maintain track task. They are denoted in percent. To understand this notation, the handling indicators distribution of the test point with medium crosswind (highlighted by a grey area in Fig. 11a, bottom part of the figure) is regarded. It has a value of 33.3%. This test point is performed three times (compare Fig. 9) and three handling indicators (as described in Sect. 4.1.3) are defined. Hence, altogether 9 handling indicators are available. Of these, three indicators have a value of 1 since the underlying limits are exceeded. The indicators for flight safety and task performance are obtained in an analogous manner.

The method used to assess the wind conditions and to find limits is relatively straightforward. First, all test points are excluded that have at least one flight safety indicator with a value of 1, or in other words a percentage of more than 0% (Fig. 11b, represented by a red cross). This is the case for the strongest gust with shorter wavelength and the strongest lateral wind shear. In the following, the task performance indicators are regarded. Only test points without indicator with a value of 1 are accepted here. Therefore, all test points that have a percentage of more than 0% are eliminated (Fig. 11c, blue cross). Hereby, the elimination of all these test points is a rather conservative approach. A definition of a higher limiting percentage would, of course, also be possible. Finally, four test points, being the medium crosswind, the shorter side gust with medium intensity, the longer side gust with low intensity and the wind shear of lowest strength, remain (Fig. 11d, green check-mark). The associated wind conditions are deemed as acceptable for fulfilling this task with the DLR HAP aircraft. It should also be noted that, for this task, the handling indicators, representing a soft criterion and therefore only serving as a support for this decision, are mainly in accordance with the exclusions made.

The respective maximum wind conditions of the remaining disturbances are

- constant crosswind of 3.0 m/s,
- side gust (33.5 m) with peak speed of 3.3 m/s,
- side gust (82.5 m) with peak speed of 1.3 m/s, and
- lateral wind shear of 0.5 m/s^2.

These values form a basis for defining the overall wind restriction limits.

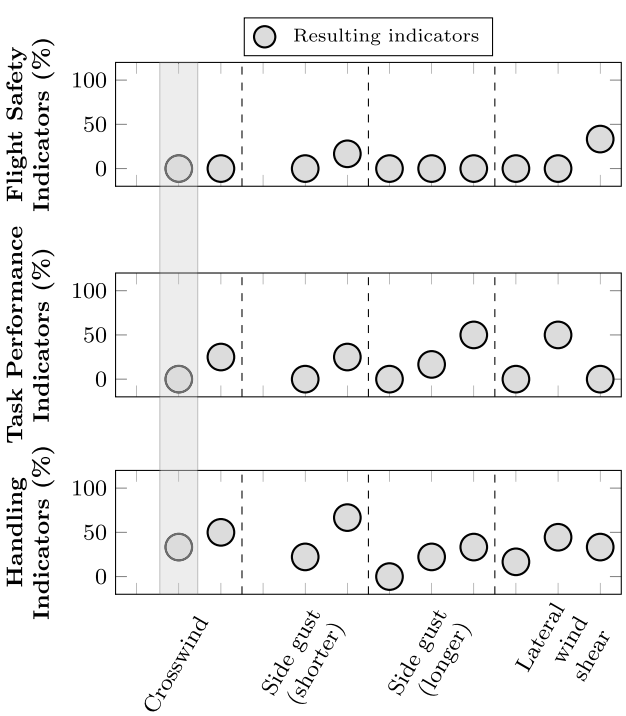

(a) All resulting indicators for the maintain track task

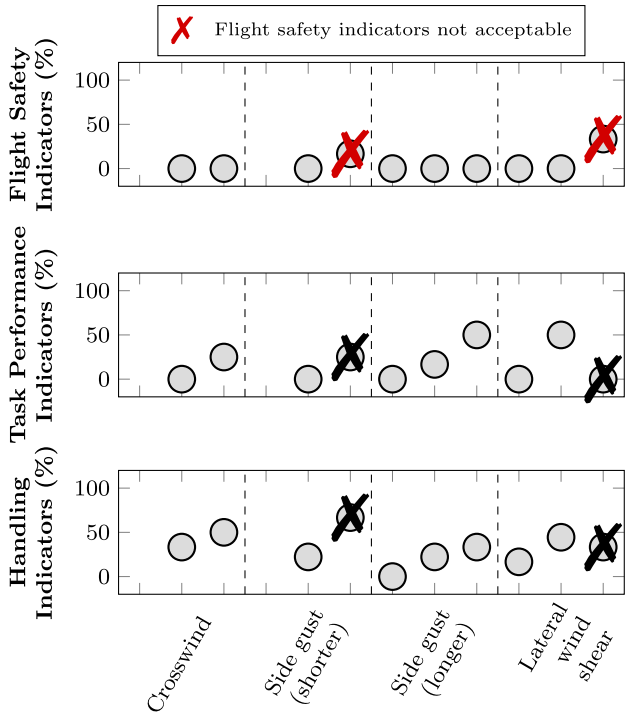

(b) Exclusion of test points due to flight safety indicators

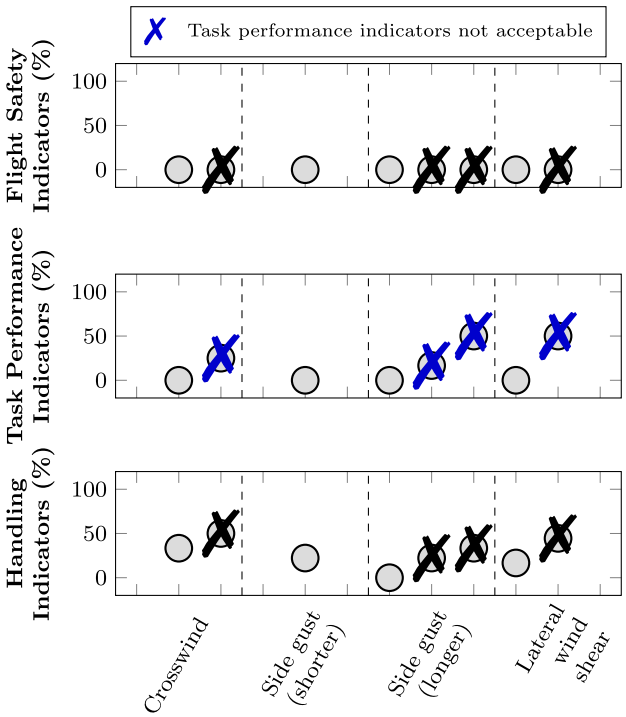

(c) Exclusion of test points due to task performance indicators

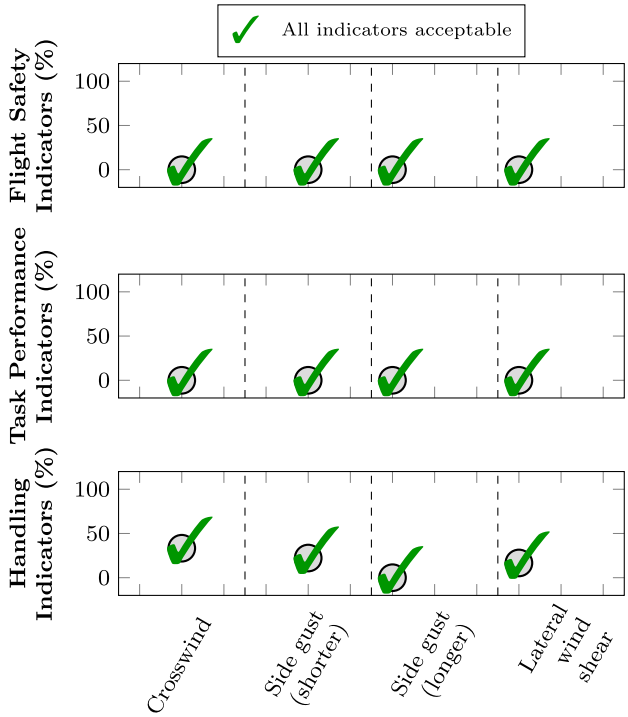

(d) Remaining test points

Fig. 11 Resulting indicators for the maintain track task and different assessment steps. The highlighted grey area in part (a) represents that the indicators belong to the same test point, which is, in this case, the maintain track task with medium crosswind. Depending on the values of the indicators for flight safety or task performance, the wind conditions of some test points are assessed as not acceptable. Note that, due to the afore-described approach to define the test program during the simulator tests based on the pilot's assessment, not all test points were performed (compare Fig. 9)

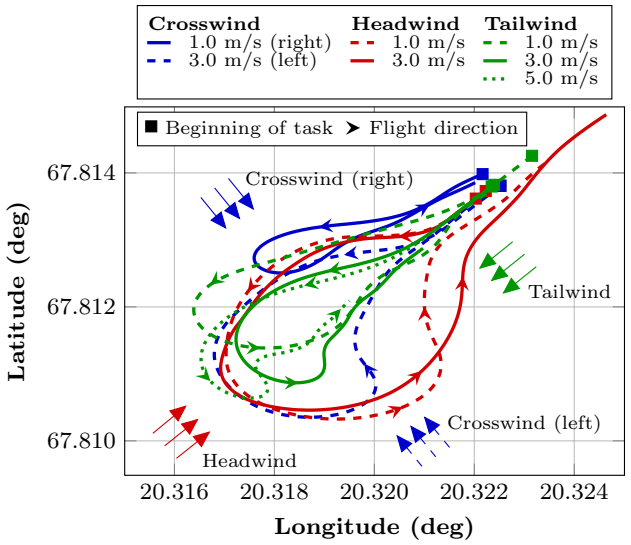

Fig. 12 Selected representative ground paths obtained during the teardrop turn task

5.2 Teardrop manoeuvre

Figure 12 provides some examples of ground paths obtained within the teardrop turn task. In addition, the respective flight directions and wind directions are plotted. The latter is applied in such a way that it is relative to the initial point, i.e. a tailwind is initially a tailwind, but will change into a crosswind and a headwind during the return. The type of wind is recognisable in the ground paths. In the cases with initial tailwind, for example, the turn tends to be more slender. In addition, the starting point is passed during the return with relatively high accuracy. The reason for this is that it is easier for the pilot to turn into the wind and to reach a destination point with a slower ground speed. For initial headwind, on the other hand, the aircraft encounters tailwind at the end of the manoeuvre. As a consequence, the starting point is slightly missed. The ground paths while crosswind is encountered are unsymmetrical. For crosswind, the flight direction plays a role. During the tests it was observed that some pilots started the manoeuvre into the wind, while others did the opposite. After finishing the task, some pilots even asked to repeat the task to try flying into the other direction. This is the reason for the higher amount of test points for this manoeuvre. Therefore, it can be concluded that there is some considerable potential for pilot training with respect to this task.

Altogether, the results show that the wind speeds, if in moderate order of magnitude, only have a minor influence on the feasibility this task. This is also reflected in the pilots' assessment and feedback. Nevertheless, this task turns out to be associated with a high workload, regardless of the wind. Figure 13 presents the handling indicators for this task. As

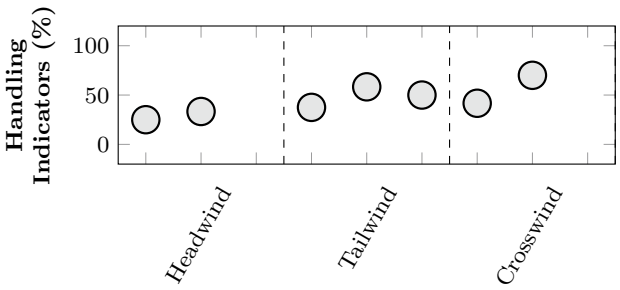

Fig. 13 Handling indicators for the teardrop turn task

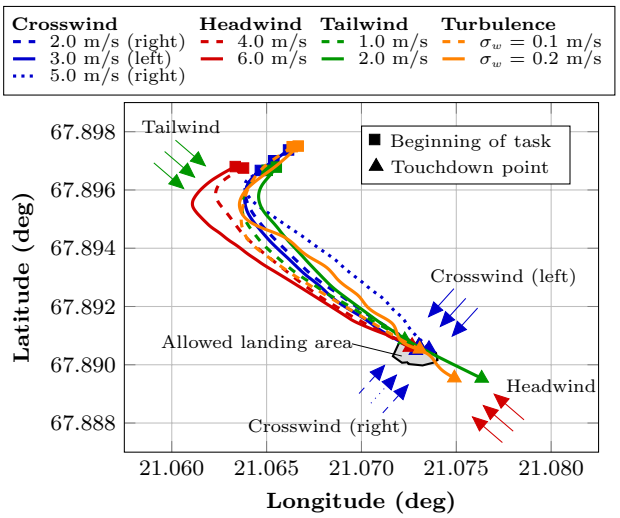

Fig. 14 Selected representative ground paths obtained during the landing task

shown, nearly all results range around 50% and have only a rather weak dependency on the wind speeds.

For this task, a constant wind speed of 3.0 m/s in any direction turns out to be acceptable.

5.3 Landing

This section deals with the results for the landing with transverse approach task. Figure 14 shows the flight paths of some selected test points. The wind directions are applied such that they are relative to the flight direction during the final approach. The figure also depicts the allowable landing area, highlighted in grey, and the respective touchdown points, marked with filled triangles. Altogether, 8 landings out of 18 were not completed in the designated touchdown area, proving that this is a very challenging task. One of the major reasons for this circumstance is the absence of air brakes and thus the low capability of the aircraft to reduce energy.

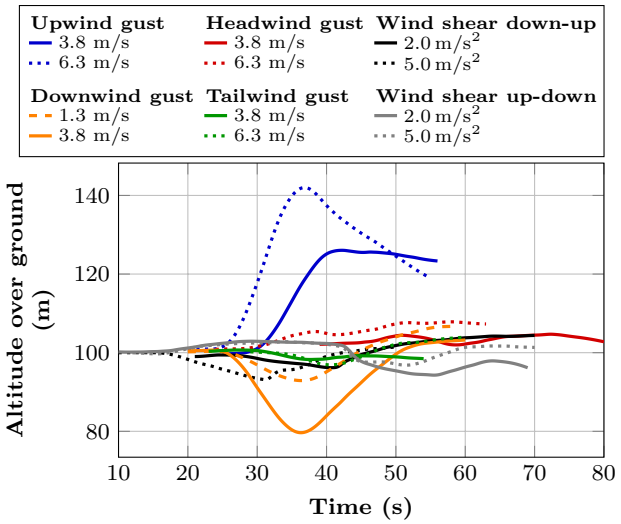

Fig. 15 Selected representative altitude profiles obtained during the maintain altitude task

In addition to the general level of difficulty, the influence of atmospheric disturbances on the feasibility of this task is strong. Cross- and tailwinds of already minor intensity hinder its successful completion significantly, while headwind, as expected, has a facilitating effect. The maximum allowable wind conditions remaining after application of the indicator assessment are

- maximum allowable crosswind of 1.0 m/s,
- maximum allowable headwind of 6.0 m/s,
- maximum allowable tailwind of 0.0 m/s, and
- standard deviation of the vertical turbulence of 0.05 m/s (with higher values for longitudinal and lateral direction according to (7)).

These results show that the landing requires, regardless of the wind condition, proper and comprehensive pilot training.

5.4 Maintain altitude

The last task presented here is to maintain altitude. The time histories for altitude over ground are presented by Fig. 15. The time slices are always cut such that they start right before the encounter of wind. This is also true for the wind shear cases.

As shown, particularly the vertical gusts are critical. The HAP aircraft is very light and tends to move with the wind rather than to show a strong dynamic response. As a consequence, the altitude changes are quite large. In addition, only limited engine power is available to counteract the downwind gusts. However, the aircraft's tendency to follow the movement of the wind field brings benefits with respect to tailwind gusts. In these cases, the presence of wind rather leads to an increase of the aircraft inertial speed than to a reduction of its airspeed relative to the wind, which would be more critical with respect to the allowed envelope. The resulting acceptable wind conditions for this task are:

- Wind shear from up to down of 2.0 m/s^2
- Wind shear from down to up of 0.5 m/s^2
- Upwind gust (33.5 m) with peak speed of 1.1 m/s
- Upwind gust (82.5 m) with peak speed of 1.3 m/s
- Downwind gust (33.5 m) with peak speed of 1.1 m/s
- Downwind gust (82.5 m) with peak speed of 1.3 m/s
- Tailwind gust (33.5 m) with peak speed of 1.1 m/s
- Tailwind gust (82.5 m) with peak speed of 3.8 m/s
- Headwind gust (33.5 m) with peak speed of 1.1 m/s
- Headwind gust (82.5 m) with peak speed of 1.3 m/s

These values form a basis for defining the overall wind restriction limits.

5.5 Resulting limits

The results presented in the previous sections are strongly linked to the limits chosen for the different indicators. They are especially tailored to the flight test campaign scheduled in the project *HAP*. In addition, the limits are chosen to be relatively conservative. Therefore, variations of the underlying limits can lead to different results. Nevertheless, the major aim of this paper is to demonstrate the method used for the assessment and to provide some exemplary results.

The results are task-dependent and based on a finite amount of different wind conditions with discrete airspeeds. While combining these results to define the overall wind restrictions, it must be taken into account that intermediate wind speeds might also be acceptable. Here, especially the handling indicators can play a key role in defining the limits. On the basis of the results, the following restrictions for a remotely piloted flight in low altitudes seem reasonable:

- Maximum allowable constant wind in any direction of 3.0 m/s while the landing must be performed such that the crosswind is lower than 1.0 m/s and no tailwind occurs
- Maximum horizontal and vertical wind shear of 0.5 m/s^2
- Horizontal gusts with maximum peak speeds of 2.0 m/s and vertical gusts with maximum peak speed of 1.5 m/s
- Continuous turbulence with a maximum standard deviation of 0.05 m/s in vertical direction (higher values in horizontal direction are allowed, which are obtained applying (7))

The resulting limits only refer to remotely piloted flights in low altitudes. For higher altitudes and flights using a flight

controller, the wind speeds of the design wind conditions still represent the acceptable limits.

6 Conclusion

In the context of this paper, virtual flight tests using a desktop simulator were carried out. Within 114 test points, three pilots performed different flight tasks with the DLR HAP aircraft under atmospheric disturbance conditions. The assessment strategy to evaluate the task performances and the criticality of the wind conditions was based on so-called indicators that showed whether underlying limits with respect to flight safety, task performance, and handling were exceeded or not.

In the tests, landing turned out to be the most challenging task while already small amounts of constant crosswind and tailwind complicated the task significantly. In contrast, the influence of constant wind on the feasibility of the teardrop turn was rather small. Concerning the maintain altitude task, vertical gusts, both upwards and downwards were the most crucial. Altogether, limiting wind conditions could be defined for the remotely piloted flight of the HAP aircraft at low altitudes. A maximum constant wind in any direction of 3.0 m/s is acceptable, whereas during landing crosswinds of 1.0 m/s must not be exceeded and tailwind must not occur. Wind shear should be limited to 0.5 m/s^2, horizontal gusts must not exceed peak speeds of 2.0 m/s and vertical gusts must have lower peak speeds than 1.5 m/s. It should be noted that these restrictions are strongly linked to the underlying limits for the indicators. Within this work, these limits were defined to be somewhat conservative.

The desktop simulator used for the tests has a relatively simple structure. This is particularly true for the vision system and the inceptor, which do not represent the real flight piloting conditions to a sufficient degree. However, the aim of this study was to investigate to which extent simple tasks could be completed by pilots during the presence of wind. In doing so, the focus was rather on the capabilities of the aircraft itself than on the conditions for the pilot. For this purpose, the simulator is deemed to be sufficient. Nevertheless, it is conceivable that some test points became more challenging for the pilots due to the shortcomings of the desktop simulator. However, in this case it can be assumed that the found limits tend to be more conservative, which would not be disadvantageous with respect to the risk mitigation for real flights. However, for pilot training, a simulator of higher quality would be required.

Latency measurements showed values around 200 ms for the reaction of the aircraft view and 300 ms for the instruments on average following a control input using the inceptor. For the flight test campaign planned within the project *HAP*, maximum values for control latency and monitoring latency of 200 ms (desirably 100 ms) each were defined as acceptable. In sum, latency values of 200 ms to 400 ms are thus to be expected in the flight test. The latencies of the used simulator are in this range. Therefore, it can be assumed that possible effects caused by latencies in the real flight are reproduced in the simulations as well.

Within the flight dynamic model used for the tests, a dynamic pressure-based quasistatic approach and aeroelastic control surface effectivenesses are used to model the flexibility of the aircraft rather than the inclusion of the structural dynamics. This signifies that effects like pilot-induced oscillations driven by the flexible dynamics cannot be reproduced in these tests. However, these are usually more relevant for higher precision tracking tasks. The focus of the works presented in this paper is rather to investigate the general feasibility of high-level tasks like flying a teardrop turn or maintaining altitude. Thus, rather low frequency inputs are required by the pilots for accomplishment. It can therefore be assumed that the structural dynamics would play a subordinated role for these tasks. Instead, the change of the aerodynamic properties due to the changing flight shape as well as the degradation of control surface effectivenesses resulting from airspeed excursions are supposed to play a major role. In can thus be concluded that for the purpose of the tests performed within these works, the aerodynamic modelling approach is accurate enough. It should however be noted, that the landing task requires a higher degree of precision. For this task, a repetition with a model that includes the structural dynamics could thus be beneficial.

In addition, the vortex lattice method, used for the aerodynamic model, is rather simple. However, especially for low airspeeds and high aspect ratios, as it is the case for the HAP aircraft, the method's accuracy is reasonable.

Overall, a high number of test points were performed in this study. However, there were a multitude of different combinations of tasks, wind conditions and wind speeds. This signifies that, for a single test point, the number of executions was rather low, most often ranging from 2 to 3. Given that the pilots had different backgrounds and a different level of experience with such a type of aircraft, the learning effect played an important role. It is supposable that, particularly at the beginning of the respective sessions, tasks were underrated because the pilots were still getting used to the aircraft's flight dynamics. Therefore, a higher number of repetitions of single test points would be desirable to further eliminate the influence of the learning effect and to support the results obtained here.

7 Future work

With respect to the designated flight test campaign, a couple of subsequent works are to be performed. First of all, further tests in the simulator need to be performed to validate the

defined limits. In doing so, the wind speeds can be adjusted with a finer discretisation around the found limits. If the tests are repeated with the same pilots, this also serves to reduce the influence of the learning effect on the consistency of the results. Moreover, tests using the flight dynamics model with the structural dynamics included, which is currently under development, will be performed. Moreover, some wind restrictions defined in this study refer to small-scale phenomena like gusts or wind shear. One important future task is to deduce requirements on larger scale meteorological conditions such that conventional weather information can be used to decide whether a flight can be performed during a certain time period or not. Finally, the setup of a more detailed simulator is planned, which will be used for comprehensive pilot training.

Acknowledgements The authors would especially like to thank the pilots that participated in the simulator study. Furthermore, the authors would like to acknowledge the colleagues involved in the project *HAP*, particularly those who are part of the flight physics team and thereby contributed in setting up the flight dynamics model used in these works.

Funding Open Access funding enabled and organized by Projekt DEAL.

References

1. National Aeronautics and Space Administration, Dryden Flight Research Center, Solar-Powered Research and Dryden, NASA Facts: FS-1998-10-0054 DFRC, available online at https://www.nasa.gov/centers/dryden/pdf/120308main_FS-054-DFRC.pdf, (1998)
2. D'Oliveira, F., Melo, F., Devezas, T.: Highaltitude platforms—present situation and technology trends. J. Aerosp. Technol. Manag. **8**, 249–262 (2016). https://doi.org/10.5028/jatm.v8i3.699
3. Ross, H.: Fly around the world with a solar powered airplane, in technical soaring. Int. J. (2008). https://doi.org/10.2514/6.2008-8954
4. Nunez, C.: Solar Impulse 2 Completes Trip Around World, Demonstrates Clean Energy and Aviation, National Geographic. https://www.nationalgeographic.com/news/2016/07/solar-impulse-completes-trip-around-world-abu-dhabi-solar-power-airplane/ (2016)
5. Stevens, P.: Zephyr: Pioneering the Stratosphere, ZP-PN-0039v2.0, Presentation, https://aaus.org.au/wp-content/uploads/2019/03/Paul-Stevens-Airbus-at-AAUS-Exploring-an-Unmanned-Future-Conference-20190225.pdf (2019)
6. Airbus Defence and Space, Airbus Zephyr, Solar High Altitude Pseudo-Satellite flies for longer than any other aircraft during its successful maiden flight, Press Release, (2018)
7. Runge, H., Rack, W., Ruiz-Leon, A., Hepperle, M.: A solar powered HALE-UAV for arctic research. In: 1st CEAS European Air and Space Conference, (2007)
8. Mohammed, A., Mehmood, A., Pavlidou, F.-N., Mohorcic, M.: The Role of High-Altitude Platforms (HAPs) in the Global Wireless Connectivity. In: Proceedings of the IEEE, **99**, 1939–1953 (2011). https://doi.org/10.1109/JPROC.2011.2159690
9. Noll, T., Brown, J., Perez-Davis, W., Ishmael, S., Tiffany, G., Gaier, M.: Investigation of the Helios Prototype Aircraft Mishap, NASA - Helios Mishap Investigation Board, (2004)
10. Australian Transport Safety Bureau, Aviation safety investigations & reports - AO-2019-056, Airbus Zephyr, (2019)
11. FlightGear Flight Simulator, https://www.flightgear.org/. Accessed Aug 2021
12. Voß, A., Handojo, V., Weiser, C., Niemann, S.: Preparation of loads and aeroelastic analyses of a high altitude, long endurance, solar electric aircraft. In: AEC2020 Aerospace Europe Conference, (2020)
13. Hasan, Y.J. et al.: Flight Mechanical Design and Analysis of a Solar-Powered High-Altitude Platform. Deutscher Luft und Raumfahrtkongress, online, (2020). https://doi.org/10.1007/s13272-022-00621-2
14. Fischenberg, D.: Identification of an Unsteady Aerodynamic Stall Model from Flight Test Data, AIAA-95-3438-CP. In: Proceedings of the AIAA Atmospheric Flight Mechanics Conference, Baltimore, Maryland, USA, (1995), pp. 138–146
15. Drela, M.: Flight Vehicle Aerodynamics. The MIT Press, New York (2014)
16. Drela, M., Youngren, H.: AVL User Primer, https://web.mit.edu/drela/Public/web/avl/
17. Voß, A., Handojo, V., Weiser, C., Niemann, S.: Results from loads and aeroelastic analyses of a high altitude, long endurance, solar electric aircraft. J. Aeroelasticity Struct. Dyn. (2022). https://doi.org/10.3293/asdj.2021.58
18. Gage, S.: Creating a Unified Graphical Wind Turbulence Model from Multiple Specifications, AIAA 2003–5529. In: AIAA Modeling and Simulation Technologies Conference and Exhibit, Austin, Texas. USA (2003). https://doi.org/10.2514/6.2003-5529
19. European Aviation Safety Agency, Easy Access Rules for All Weather Operations (CS-AWO), (2018)
20. Council, N., Sciences, D., Systems, C., Safety, C.: Aviation Safety and Pilot Control: Understanding and Preventing Unfavorable Pilot-Vehicle Interactions. National Academies Press, Washington, D.C. (1997).. (**ISBN: 9780309056885**)
21. Mandal, T., Gu, Y., Chao, H., Rhudy, M.: Flight data analysis of pilot-inducedoscillations of a remotely controlled aircraft. In: AIAA Guidance, Navigation, and Control (GNC) Conference, ser. AIAA Guidance, Navigation, and Control (GNC) Conference, (2013) **ISBN 9781624102240**
22. Mandal, T.K., Gu, Y.: Analysis of pilot-induced-oscillation and pilot vehicle system stability using UAS flight experiments. Aerospace 3(4), (2016) **ISSN: 2226-4310**
23. European Aviation Safety Agency, Certification Specifications for Large Aeroplanes—CS-25, Amendment 3, (2007)